Final Report for NAG 2-1269

Measurements of Nucleation-Mode Particle Size Distributions
in Aircraft Plumes during SULFUR 6

27 December 1999

Charles A. Brock
Associate Research Professor
Department of Engineering
University of Denver
2390 S. York St.
Denver, CO 80208
(303) 871-3046
(303) 871-4405 (fax)
cbrock@du.edu

Deborah G. Bradford
Research Administrator
Office of Sponsored Programs
University of Denver
2199 S. University Blvd.
Denver, CO 80208
(303) 871-4040
(303) 871-2623
dbradfor@du.edu

Introduction

This report summarizes the participation of the University of Denver in an airborne measurement program, SULFUR 6, which was undertaken in late September and early October of 1998 by the Deutsches Zentrum für Luft- und Raumfahrt (DLR). Scientific findings from two papers that have been published or accepted and from one manuscript that is in preparation are presented.

The SULFUR 6 experiment was designed to investigate the emissions from subsonic aircraft to constrain calculations of possible atmospheric chemical and climatic effects. The University of Denver effort contributed toward the following SULFUR 6 goals:

- To investigate the relationship between fuel sulfur content (FSC--mass of sulfur per mass of fuel) and particle number and mass emission index (EI--quantity emitted per kg of fuel burned).
- To provide upper and lower limits for the mass conversion efficiency (η) of fuel sulfur to gaseous and particulate sulfuric acid.
- To constrain models of volatile particle nucleation and growth by measuring the particle size distribution between 3 and 100 nm at aircraft plume ages ranging from 10^{-1}-10^{3} s.
- To determine microphysical and optical properties and bulk chemical composition of soot particles in aircraft exhaust.
- To investigate the differences in particle properties between aircraft plumes in contrail and non-contrail situations.

The experiment focused on emissions from the ATTAS research aircraft (a well characterized, but older technology turbojet) and from an in-service Boeing 737-300 aircraft provided by Lufthansa, with modern, high-bypass turbofan engines. Measurements were made from the DLR Dassault Falcon 900 aircraft, a modified business jet.

The Atmospheric Effects of Aviation Program (AEAP) provided funding to operate an instrument, the nucleation-mode aerosol size spectrometer (N-MASS), during the SULFUR 6 campaign and to analyze the data. The N-MASS was developed at the

2

University of Denver with the support of NOAA's Office of Global Programs and NASA's AEAP and measures particle size distributions in the 4-100 nm range.

Funding was provided for the following specific tasks:

1. Preparatory work. Design and build brackets to mount the N-MASS in the Falcon rack-mount system. Purchase an LCD monitor for display in the Falcon cabin, and modify software to synchronize time with other instruments.
2. Ship the N-MASS and support and calibration equipment to DLR and perform physical integration onto the Falcon.
3. Participate in detailed calibrations of the N-MASS and DLR CNCs. Generate particles and separate them into known sizes using a differential mobility analyzer supplied by DLR. Use a highly sensitive electrometer and filter/Faraday cup system to provide an absolute calibration standard for the singly charged particles. Calibrate the sample flow rate as a function of instrument pressure and test calibration drift over simulated flight pressure conditions.
4. Participate in the SULFUR 6 flight series from 23 September to 2 October 1998.
5. Cooperate with other researchers to integrate the varied data (*e.g.*, GPS, CO_2, $H_2SO_4(g)$, chemi-ions, particle size distributions and compositional information) and numerical simulations and publish the results.

Each of the above tasks was successfully completed.

The remainder of this report summarizes the accomplishment of tasks (3) to (5) above, and reports the scientific findings resulting from the calibrations, measurements, and analysis. Some results from SULFUR 6 have been published by Petzold *et al.* (1999) and accepted for publication (Schröder *et al.*, 2000), while a third manuscript (Brock *et al.*, 2000) will be submitted soon. Portions of this report have been extracted from the Brock *et al.* manuscript.

Summary of Results

Calibration and Evaluation of Uncertainties

With the notable exception of the SNIF experiments (Anderson *et al.*, 1998, Cofer *et al.*, 1998), many past efforts at evaluating particle production from flying aircraft have been hampered by poorly evaluated experimental uncertainties and biases. For SULFUR 6, we expended considerable effort to ensure that the particle measurements had carefully characterized experimental uncertainties.

Measurements of particle concentration were made using 9 particle counters operating in parallel. These instruments, condensation nucleus counters (CNCs), detect and count particles larger than a minimum size by condensing a working fluid (usually n-butyl alcohol) on the small particles and growing them to droplets that are easily counted. The minimum detectable diameter is controlled by the supersaturation and growth time within the condenser of the instrument. The supersaturation and growth times may be controlled by varying the geometry, temperature, and/or flow rate of the condenser and/or by changing the working fluid. Each of the CNCs used in this study operated with a different supersaturation by adjusting these parameters, and thus had different minimum detectable diameters.

Five of the CNCs were housed in a single instrument, the University of Denver's nucleation-mode aerosol size spectrometer (N-MASS) [Brock *et al.*, 2000]. The 5 CNCs within this instrument operate in parallel at a fixed pressure of 60 mb downstream of a critical orifice. The remaining 4 CNCs, operated by DLR, were placed in parallel with the N-MASS; all instruments sampled continuously from a single inlet (Fig. 1). After entering the aircraft, the sample flow (with very high concentrations) was diluted by a factor of 22:1 (±17%) with filtered ambient air. The instruments exhausted to a venturi exit, and were operated internally at a measured pressure slightly lower than the ambient value. Convective heat transfer between the aircraft cabin and the sampling tubing resulted in a heating of the sample flow to near cabin temperature.
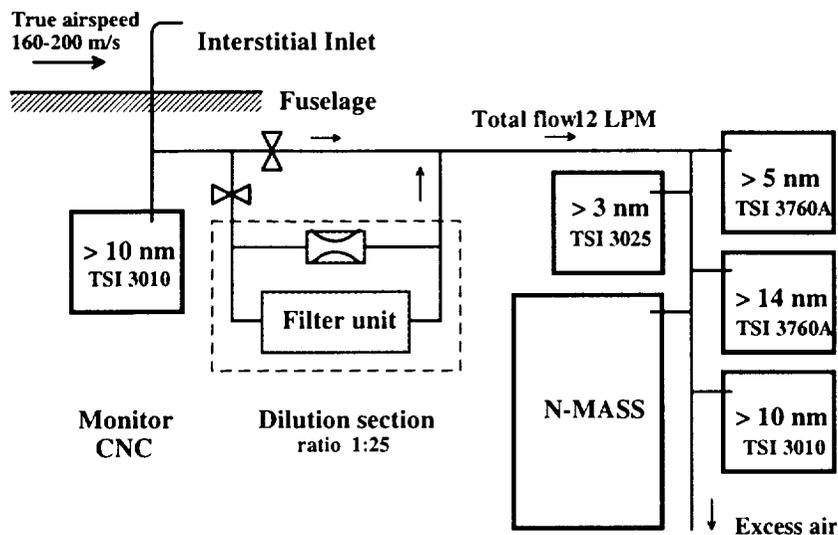
Figure 1. Schematic of the aerosol sampling system used aboard the Falcon during SULFUR 6 [Schröder *et al.*, 2000]. The backward oriented interstitial sampling inlet was mounted on top of the cabin, approximately 3 m behind the cockpit and about 35 cm from the fuselage. After passing (an optional) dilution section (ratio 22:1) the aerosol sample was directed towards the CNCC and the N-MASS systems.

On the day after the measurements, the particle instrument package was calibrated in the laboratory (Fig. 2). Particles of $(NH_4)_2SO_4$ were produced by condensation following evaporation in a tube furnace. The particles were classified in a differential mobility analyzer (DMA, Model 3071A, TSI, Inc., St. Paul, MN USA) to produce a nearly monodisperse, singly charged, calibration aerosol. This calibration aerosol was diluted and introduced simultaneously into the aircraft sampling tubing and into a Faraday cup attached to an electrometer. The electrometer provides a fundamental measurement of the concentration of particles produced by the DMA. However, because a relatively high concentration of particles was required to produce a significant signal on the electrometer, it was not used as the primary calibration reference. Instead, a TSI Model 3025A ultrafine particle counter, which was part of the flight package, was used as the standard against which the other instruments were calibrated. Over a range of particle sizes from 6 to 60 nm, the ultrafine particle counter and the electrometer agreed linearly to within 2% following corrections to the TSI data for diffusion losses and particle-in-beam coincidence (Fig. 3). Because calibration aerosol with $D_p < 4$ nm could not be
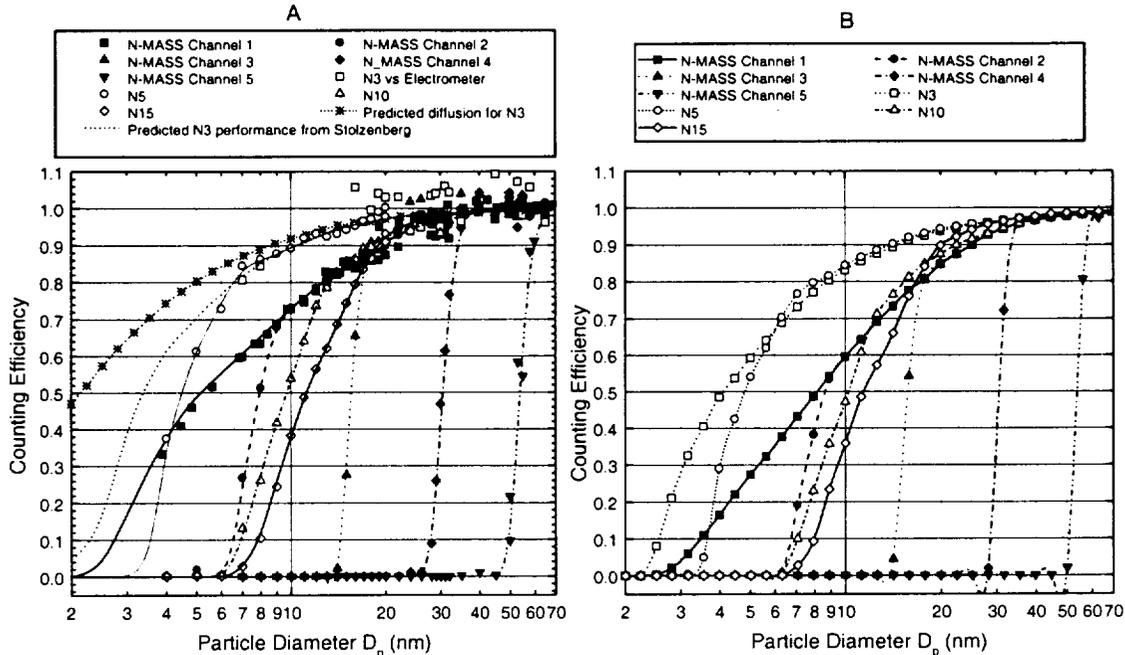
5

Figure 2. A) Measured detection efficiency of the DLR CNCs (N5, N10 and N15) and the five channels of the University of Denver N-MASS, using the aircraft tubing system, as a function of particle diameter D_p at a pressure of 960 mb, relative to the N3 instrument (a TSI 3025A). The points are experimental data and the lines are fits to the data. Points for the N3 (TSI 3025A, the reference instrument) are relative to an electrometer. Calculated diffusion losses within the tubing leading to the N3 instrument are shown, as is a calibration for this instrument (with diffusion losses added) as determined by Stolzenburg and McMurry [1991], which extends to smaller sizes than we achieved in our experimental configuration. The calibration aerosol is composed of $(NH_4)_2SO_4$. B) Calculated response of the instruments in (A) at 321 mb operating pressure, based on the fitted curves in (A) and calculated diffusion losses within the sampling system at the measurement pressure.

produced, the calibration curves for smaller diameters are extrapolated (for N-MASS channel 1 and N5) or based on published data (for N3, see Stolzenburg and McMurry [1991]).

The calibration of the 9 CNCs shows sharp cut-off characteristics for particles with diameters (D_p) greater than about 13 nm, and more gradually sloping curves for particles with smaller D_p (Fig. 2). This sloping response is due to substantial diffusion losses in
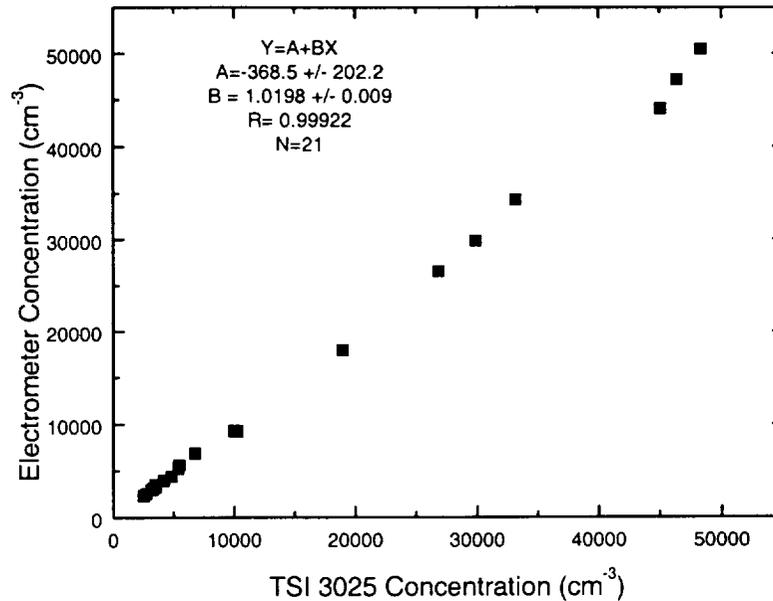
6

Figure 3. Counting efficiency of the TSI Model 3025 CNC used as the calibration reference standard as established against the primary standard, a Faraday cup and electrometer.

the sampling tubing and, particularly for the N-MASS for $D_p<10nm$, within the instruments themselves. Diffusion losses in incompressible, fully developed, laminar pipe flow increase as pressure decreases and are readily calculated. Based on the measured tubing lengths and known volumetric flows of the instruments, diffusion losses in the sampling lines have been calculated as a function of D_p for the calibration pressure (960 mb) and the three principal in-flight sampling pressures (approximately 450 , 320 and 205 mb inside the instruments). These diffusion losses have been incorporated into the algorithm used to calculate the size distribution from the CNC measurements, as described below. We note that the diffusion calculations do not account for losses in the tubing bends, where radial velocity components can increase diffusional deposition to the walls. Particle losses due to inertial deposition are negligible for the D_p (<50nm) considered here and the flowrates and radii of curvature in the sampling tubes.

The calibration shown in Fig. 2 is for an aerosol composed of $(NH_4)_2SO_4$. There is evidence of a shift in the response function of the CNCs that use n-butyl alcohol as the working fluid when the calibration aerosol is composed of NaCl instead of $(NH_4)_2SO_4$. [Schröder et al., 2000]. The N-MASS, which uses perfluorotributylamine $(CF_3(CF_2)_3)_3N$ --an hydrophobic, inert compound--as the working fluid, has not shown a detectable sensitivity to particle composition in laboratory tests with NaCl, $(NH_4)_2SO_4$, H_2SO_4 and Ag particles. For the butanol-based CNCs, however, differences in the instrumental response between the laboratory calibration aerosol and the aircraft-produced particles remains a potential bias.

Method to determine the particle size distribution

From the measurements of concentration from the multiple parallel CNCs used in SULFUR 6, we wish to determine the size distribution of particles in the plumes of flying aircraft. These size distributions can be used to calculate the number, surface area and volume concentration of particles within a given size range, which can then be related to the sulfur content of the fuel and other controlling parameters. One approach that has been used in the past to determine differential size distributions [e.g., Schröder et al.] is to subtract the concentrations of adjacent CNCs, and assign the resulting concentration to the size interval lying between the nominal 50% size cut diameters of the CNCs. For the data presented here, this method can be used quantitatively only for particles with $D_p>12$ nm [Petzold et al., 1999]. For smaller particle diameters, the sloping--and even crossing-- response functions argue against such an approach.

An alternative method, used here, is to make use of an inversion technique to determine a smooth, non-negative particle size distribution function that is consistent with the responses measured simultaneously by the parallel CNCs. Each of the CNCs i records a single number X_i,

$$X_i = \int_0^\infty N(D_p) K_i(D_p) \, dD_p, \tag{1}$$

8

where N is the particle size distribution function (the number of particles occurring between particle diameters D_p and $D_p + dD_p$), and $K_i(D_p)$ is the response function of instrument i to a particle of size D_p (Fig. 2). Note that the $K_i(D_p)$ vary as a function of pressure due to changing diffusion losses in the sampling system. The inverse problem is, given $K_i(D_p)$ known with experimentally characterized uncertainty, and X_i measured with known uncertainty, what is $N(D_p)$? We solve a finite difference approximation of (1) for $N(D_p)$ using a version of the smoothed Twomey (ST) algorithm [Markowski, 1987]. This constrained nonlinear inversion technique is used to generate a 33-point representation of $N(D_p)$ for $2 \le D_p \le 80$ nm. An infinite number of possible $N(D_p)$ that satisfy (1) exist, most characterized by oscillations of a scale smaller than the diameter difference between adjacent CNC channels. The ST method uses a nonlinear technique to choose one smooth, non-negative solution that does not contain these high frequency modes. The algorithm accounts for the sloping, crossing nature of the response functions and produces a size distribution that is consistent with the concentrations measured by each CNC. The algorithm minimizes, to within experimental uncertainty, a chi-squared value related to the difference between the predicted and actual instrument response through an iterative weighting scheme. Variants of the ST algorithm have been used to recover size distributions from diffusion batteries [Markowski, 1987], impactors [Winklmayr et al., 1990], and optical particle counters [Jonsson et al., 1995].

Analysis of uncertainties

We have identified three primary sources of uncertainty in the measurements and analysis. These uncertainties are summarized in Table 2. The first of these is a random uncertainty due to the precision of the measurement of particle emission indices. This uncertainty stems from measurement precision of the particle concentrations measured by the multiple CNCs (which are dominated by flow uncertainties and counting statistics), uncertainty in integrating the measurements over a fixed time period in the plume, uncertainty in determining the FSC, and uncertainty in determining the dilution factor within the plume based on CO_2 and/or temperature measurements. The second type of

uncertainty includes possible systematic errors, such as sampling biases due to inertial segregation at the rear-facing sampling inlet, improper estimation of diffusional losses in curved tubing, and errors in the response curves of the CNCs due to extrapolation of calibration data for $D_p<4$ nm.

The third source of uncertainty stems from the inversion algorithm applied to determine the particle size distribution function. A user-defined smoothing parameter is used to limit high-frequency oscillations of the solution. This smoothing parameter has been chosen based on laboratory studies using the 5-channel N-MASS and a scanning mobility

Table 1. Sources of random (class=R), systematic (class=S) and numerical (class=N) uncertainties in determining particle number EI*. Uncertainties are 1-sigma values.

Class	Source	Estimated Magnitude	Comments
R	Instrument flow uncertainty	±8%	See calibration scatter (Fig. 2)
R	Calibration reference	±5%	Electrometer and N3 uncertainties
R	Counting statistics	<1% N3; <10% N-MASS chan 5	Good statistics in plumes
R	Plume dilution	±12%	Dilution calculated from CO_2. Applies equally to all CNC channels for a given plume crossing.
R	Plume integration	±20%	Applies equally to all CNC channels for a given plume crossing.
R	Sample dilution	±15%	Applies equally to all CNC channels for a given plume crossing.
R	Linear propagation of above random errors	±28%	For dilution and integration only; other errors accounted for in Monte Carlo simulation
S	Inertial segregation at sampling inlet	± 5%	Small error for Dp < 50 nm; see Schröder et al. [1998]
S	Enhanced diffusion losses in tubing bends	- 5%	Small fraction of total diffusion losses.
S	Extrapolation of calibration curves	± 50%	Significant possible bias at very small particle sizes; sign of bias unknown.
N	Choice of smoothing parameter and propagation of other uncertainties in inversion	±26%	Calculated for $D_p<10$ nm. Only first 3 random uncertainties listed above (which apply randomly to each channel) are considered.

Table 2. Propagation of total random uncertainties, including numerical uncertainties, (Table 2) to the final number, surface and mass EI^* data products. A random shift of ± 5% in the D_p of the response curves has also been added to the Monte Carlo simulation of numerical uncertainties in surface and volume to account for possible bias in the D_p of the calibration aerosol. Uncertainties are 1-sigma values. Note that possible systematic uncertainties become important when the size distribution is heavily weighted to particles with D_p < 5 nm, and must be incorporated in the interpretation of the data.

Parameter	Magnitude of Uncertainty
Number EI^*	38%
Surface EI^*	36%
Mass EI^*	38%[†]

[†]Includes 11% uncertainty in determining fuel sulfur content at 2.6 ppmm.

particle sizer. To constrain the uncertainty introduced by this choice of smoothing parameter, and to evaluate how experimental precisions propagate through the data inversion, we have performed a Monte Carlo sensitivity test. The results of this test (Table 2), coupled with the integration and dilution uncertainties, indicate that particle number, surface and mass EI^*'s are determined with one-standard-deviation uncertainties of ±38%, ±36% and ±38%, respectively. This analysis excludes the possible biases (the S-class uncertainties) noted in Table 1.

Measurements

Data were obtained from two flights, one behind the ATTAS aircraft (with RR M45H M501 engines) and one behind the Lufthansa B737-300 (with CFM56-3B1 engines). Both flights included measurements at different altitudes under non-contrail-forming and contrail-forming conditions at distances as close as ~35 m behind the leading aircraft, or 0.15 seconds plume age. The aircraft flew at normal operating speeds at flight level (FL) 190, 260, and 350-370 (5.8, 7.9 and 10.7-11.3 km above sea level, respectively). Both aircraft were supplied with fuel with a FSC of only 0.8 ppmm as measured at the source. Following transport in a tanker truck, fueling of the aircraft, and flight, a sample taken from the aircraft tank contained a FSC of 2.6 ± 0.3 ppmm FSC. Fuel containing 118 and 56 ppmm S was flown in another fuel bladder on the ATTAS and B737-300, respectively.

56 ppmm S was flown in another fuel bladder on the ATTAS and B737-300, respectively. In flight, engines could be operated from either fuel source independently or simultaneously.

Results

The data collected in SULFUR 6 have been analyzed with a focus on three issues. In Petzold *et al.* (1999), measurements of the soot particles produced by the ATTAS and B737-300 have been combined with data from other field projects. Factors controlling apparent volatile particle number emission index (EI, number of particles produced per kg of fuel consumed) are the subject of the recently accepted work by Schroeder *et al.* (2000). The size distributions of the volatile particles observed in the B737 plume and the apparent particle mass EI are the subjects of the manuscript by Brock *et al.* (2000). The major findings from these analyses that are derived from the N-MASS measurements include:

1) The mass and number EIs of soot particles from the ATTAS and B737-300 are in close agreement with earlier measurements from the ATTAS and more modern aircraft. for the B737 with CFM56-3B1 engines, the number and mass EIs of soot were 3.5×10^{14} kg^{-1} and 0.011 g kg^{-1}, respectively.

2) The number mean diameter of the primary soot mode--as determined by the spherical-particle-calibration of the CNCs and N-MASS--is 25 nm with a geometric standard deviation of 1.55. These values are in general agreement with previous ground-based and airborne results, and strongly suggest that engine test cells and ground run-ups are reasonable surrogates for airborne measurements of soot number and mass EI. Note, however, that the condensation of organic and sulfur compounds onto the soot surface--which may significantly chemical reactivity and cloud nucleating ability of the particles--may be very different in flight than on the ground.

3) The size and apparent EI of the volatile particle mode varies as a function of FSC and plume age (Figs. 4, 5). For FSCs < 100 ppmm, as was used in SULFUR 6, the mode peaks are smaller than 4 nm. The size distribution of such nano-particles is very difficult to measure as it lies near the bottom limit of particle detectable with CNCs (Fig. 3). As a result, the EIs for these particles have relatively large uncertainties (Tables 1, 2). For a FSC of 2.6 ppmm, the apparent conversion efficiency of sulfur in fuel to sulfur in particles, η^*, assuming a composition of H_2SO_4/H_2O, is 23 ± 14 %. For the 56 ppmm FSC case, η^* is $3.3 \pm 2.1\%$. It is likely that, for the 2.6 ppmm case, a significant fraction of the particle mass is not composed of condensed sulfur compounds, but rather of low-vapor-pressure organic compounds.

4) When fuels with very low sulfur content (e.g., 2.6 ppmm) are used, copious quantities of particles with diameters < 4 nm are still measured in the plume, with apparent number EIs $\sim 10^{-17}$ kg^{-1} (Fig. 4). Schröder et al. (2000) suggest that a relatively constant number of particles are produced in the first few milliseconds after emission, and that this EI is governed by the production of chemi-ions in the engine. Even in the absence of significant fuel sulfur, some (presumably) organic species condense on the charged molecular clusters and produce a measurable particle concentration.

5) The very wide range of apparent particle EIs evident in the literature is almost certainly caused in part by variations the growth of the sub-5 nm particles, which will increase with increasing FSC and plume age. Contributing to this variability is the range of different instruments used to measure the apparent particle EI. Most instruments do not measure particles with diameters < 10 nm with perfect efficiency. Given the sharply increasing particle concentration with decreasing diameter evident in the data presented here, it is clear that small variations in the response functions of CNCs or wire impactors could result in vastly different estimates of apparent particle number and mass EI.
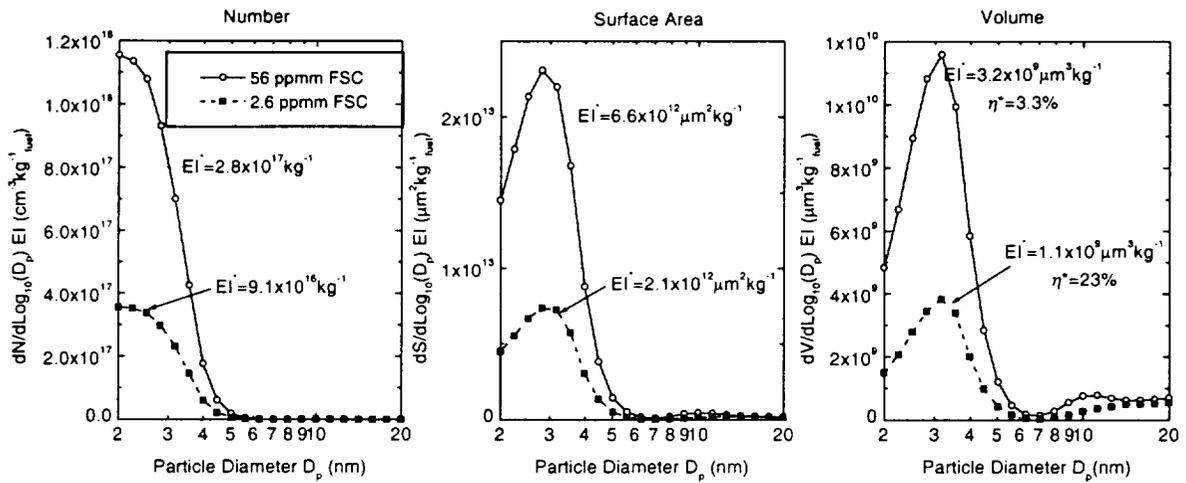
Figure 4. Differential number, surface area and volume particle size distribution EI* determined from numerical inversion of the concentrations measured with 9 CNCs about 90 m behind a B737-300. Units are in differential value per kg of fuel burned. The scaling of the ordinate is linear, so that an integral under the curve is the EI* of that parameter over the integrated size range. Note that a significant portion of the EI*s appears to fall in particles with $D_p < 2.8$ nm, the minimum detectable diameter of the CNCs; the curve from 2 to 2.8 nm is extrapolated from the numerical inversion.
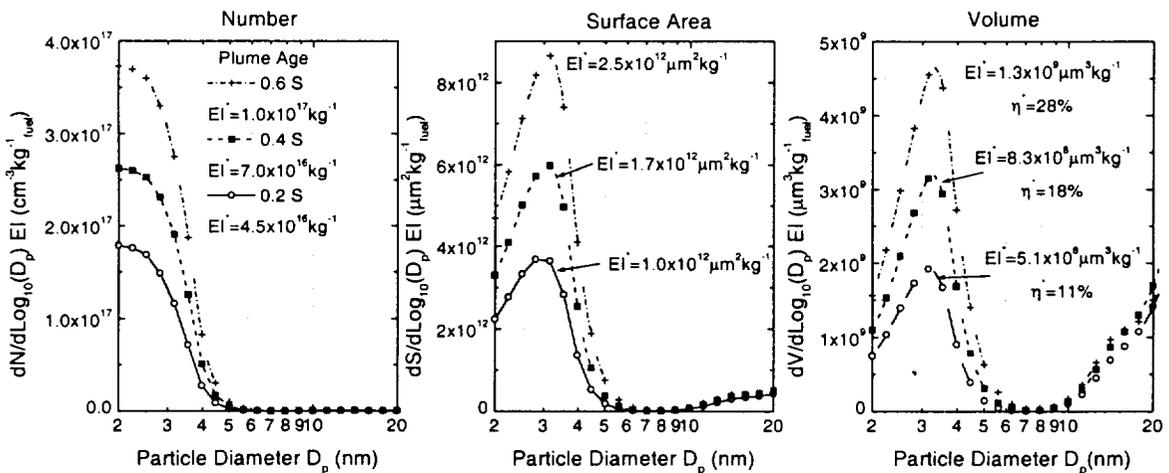

Figure 5. As in Fig. 4, but for three plume ages (200, 400 and 600 ms) while the B737-300 burned fuel with 2.6 ppmm sulfur content. Note the increasing apparent emission indices (EI*s) as a function of plume age. These values approach a constant level asymptotically at a few seconds plume age (Schröder et al., 2000).

14

6) The values of η^* found in SULFUR 6 differ from the results reported for the stratospheric Concorde intercepts (Fahey *et al.*, 1995), where $\eta^* \geq 12\%$ for a FSC of ~300 ppmm. The differences in the values of η^* for the two cases may be caused by: a) significantly larger emissions of SO_3 from the Concorde engines than from the B737-300 engines; b) significantly greater emissions of condensable organic compounds from the Concorde than from the B737-300; c) a large error in the understanding of the response of the CNCs used in the Concorde study, which requires a substantial flaw in multiple laboratory calibrations of the same type performed during SULFUR 6; or d) an unidentified in-flight change of the CNC response during the Concorde study.

Conclusions

The N-MASS instrument was combined with the DLR CNCs and supporting instruments to provide measurements of particle production in aircraft exhaust with unprecedented resolution and accuracy. The data strongly indicate that, for FSCs exceeding ~50 ppmm, only a few percent of the sulfur emitted from modern subsonic aircraft rapidly forms small particles. Extrapolating this finding to possible future supersonic aircraft cannot be accomplished without a clear understanding of the discrepancy between the Concorde observations and those of more modern aircraft. Such an understanding requires detailed knowledge of the mechanisms of sulfur oxidation in the combustor, turbine and exhaust of aircraft engines--information which now is lacking.

Analysis of data from the mass spectrometer operated by Prof. Dr. Frank Arnold of the University of Heidelberg has not yet been published, but should provide limits to the concentration of chemi-ions produced by the ATTAS and Boeing 737 aircraft. The analysis of the particle size distributions is continuing in cooperation with Dr. Fanqun Yu

of the University of California at Los Angeles and Dr. Bernd Kärcher of DLR Oberpfaffenhofen, who are running numerical models of chemi-ion-assisted particle formation and growth (*e.g.*, Yu and Turco, 1997; Kärcher *et al.*, 1998). The detailed size distributions recorded in the aircraft plumes provide a very strong constraint for evaluation of these models and should be sufficient to disprove the chemi-ion hypothesis if it is substantially incorrect.

References

Anderson, B. E., W. R. Cofer, J. W. Barrick, D. R. Bagwell and C. H. Hudgins, Airborne observations of aircraft aerosol emissions, 2, Factors controlling volatile particle production, *Geophys. Res. Letts.*, **25**, 1693-1696, 1998.

Brock, C. A., D. W. Gesler, M. J. Reeves, B. G. Lafleur and J. C. Wilson, A new instrument for fast-response measurements of particle size distributions in the 4-60 nm diameter range. To be submitted to *Aerosol Sci. Technol.*, 2000.

Brock, F. Schröder, A. Petzold, M. Fiebig, R. Busen, and R. Baumann, Observations constraining the formation of particles in aircraft exhaust. To be submitted to *J. Geophys. Res.*, 2000.

Cofer III, W. R., B. E. Anderson, E. L. Winstead and D. R. Bagwell, Calibration and demonstration of a condensation nuclei counting system for airborne measurements of aircraft exhausted particles, *Atmos. Environ.*, 1998.

Jonsson, H. H., Wilson, J. C., Brock C. A., Knollenberg, R. G., Newton, R., Dye, J. E., Baumgardner, D., Borrmann, S., Ferry, G. V., Pueschel, R., Woods, D. C., Pitts, M. C., Performance of a focused cavity aerosol spectrometer for measurements in the stratosphere of particle size in the 0.06-2.0 µm Diameter Range, *J. Atmos. Oceanic Technol, 12:115-129*, 1995a.

Kärcher, B., F. Yu, F. P. Schröder, and R. P. Turco, Ultrafine aerosol particles in aircraft plumes: Analysis of growth mechanisms, *Geophys. Res. Letts.*, **25**, 2793-2796, 1998.

Markowski, G. R., Improving Twomey's algorithm for inversion of aerosol measurement data, *Aerosol Sci. Technol.*, **7**, 127-141, 1987.

Petzold, A., A. Döpelheuer, C. Brock, and F. Schröder: In-situ observations and model calculations of black carbon emission by aircraft at cruise altitude, *J. Geophys. Res.*, *104*, 22171- 22181, 1999.

Schröder, F., C. A. Brock, R. Baumann, A. Petzold, R. Busen, P. Schulte, M. Fiebig, *In-situ* studies on volatile jet exhaust particle emissions - Impacts of fuel sulfur content and thermodynamic conditions on nuclei-mode aerosols, accepted for publication in *J. Geophys. Res.*, 2000.

Stolzenburg, M. R., and P. H. McMurry: An ultrafine condensation nucleus counter. *Aerosol Sci. Technol.*, *14*, 48-65, 1991

Yu, F. and R. P. Turco, The role of ions in the formation and evolution of particles in aircraft plumes, *Geophys. Res. Letts.*, **24** 1927-1930, 1997.